Microplastic trapping in dam reservoirs driven by complex hydrosedimentary processes (Villerest Reservoir, Loire River, France)

E. Dhivert, Ngoc-Nam Phuong, Brice Mourier, C. Grosbois, Johnny Gasperi

Author Accepted Manuscript. Water Research, Available online 1 October 2022
https://doi.org/10.1016/j.watres.2022.119187

Microplastic trapping in dam reservoirs driven by complex hydrosedimentary processes (Villerest Reservoir, Loire River, France)

Dhivert E. [(1)], Phuong N., N. [(2)], Mourier B. [(3)], Grosbois C. [(1)], Gasperi J. [(2)]

1) University of Tours, EA 6293 GéoHydrosystèmes continentaux, F-37200 Tours, France

2) University Gustave Eiffel, GERS-LEE, F-44344 Bouguenais, France

3) University of Lyon, University Claude Bernard Lyon 1, CNRS, ENTPE, UMR 5023 LEHNA, F-69518, Vaulx-en-Velin, France

Corresponding author: johnny.gasperi@univ-eiffel.fr

Highlights:

- Reservoir bottom with a coarse- to fine-grained sediment gradient
- Microplastic abundance is higher in fine-grained sediments
- Higher diversity of polymers identified in fine-grained sediments
- Microplastic particle size not related to sediment grain size
- Polymer partition may be driven by their density during the settling process

Graphical abstract:

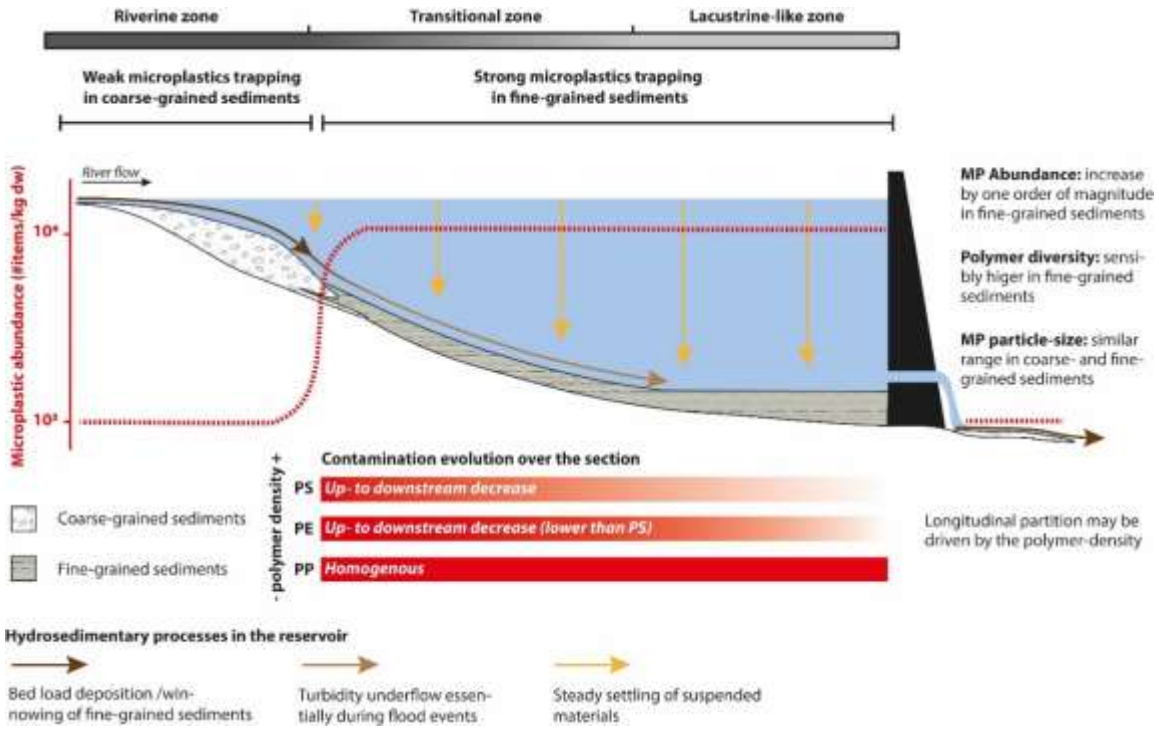

Abstract:

Dam reservoirs can strongly influence the spatial distribution of sediment pollution by microplastics (MP). The Villerest reservoir (Loire River, 36 km long) is a good candidate to study the relationship between MP pollution and hydrosedimentary processes. Sediments were collected from the dam-controlled river section and from 3 km downstream. Geomorphological and sedimentological analyses were performed and microplastics were analysed using µFTIR imaging (polymer identification for particle sizes ≥ 25 µm). This paper highlights strong MP levels (on an order of 10^4 items/kg dw) over the section characterized by fine-grained sediments (FGS). In coarse-grained sediments (CGS), at the upstream part of the reservoir and downstream of the dam, levels are one order of magnitude lower. FGS are indicator of long-time settling processes. Such conditions lead to foster the MP trapping as low-density suspended materials in the water column. CGS deposits originate from the river bed load. These sediments are transported in high-velocity and high-turbulent flow conditions. Moreover, post-depositional reworking of the finest fraction can occur according to hydrofluctuations. Here are adverse conditions for the MP trapping. The polymer diversity is also higher in FGS than in CGS. However, the range of plastic particle sizes is similar in FGS and CGS and is not related to the sediment grain-size distribution. Moreover, in both FGS and CGS, the polymer abundance is not correlated with the grain-size distribution or with the organic matter content. In the reservoir context, a change in the polymer partition appears over the FGS section in the downstream direction, depending on the polymer density. From a fundamental point of view, this work contributes to improving our understanding of the key role played by hydrosedimentary processes in MP repartition. These findings also have operational scopes, providing significant elements to advocate for a better consideration of MP pollution during sediment management operations.

Key words:
Microplastic, Dam reservoir, Sediment, µFTIR imaging, Grain-size analysis

1. Introduction

Beyond their role as pathways from plastic sources to the ocean, rivers also constitute sinks for plastic debris, affecting environmental quality and biodiversity (Waldschläger et al., 2020, van Emmerik et al., 2022).

Microplastic pollution (MP, particle-sized plastic ranging between 1 µm and 5 mm) has risen in interest in dam reservoirs because high levels are often reported (Guo et al., 2021). Reservoirs can foster MP accumulation in the sediment compartment (e.g., Di and Wang, 2018; Watkins et al., 2019, Wu et al., 2022). Such a trapping effect was also described for other pollutants because reservoirs constitute preferential settling environments for the finest fraction of sediments and associated chemicals (e.g., Bertrand et al., 2015 for PAH, Rapin et al., 2020 for phosphorus; Culicov et al., 2021 for trace elements and lanthanides). MPs are particle pollutants; they take part in the solid transport which is largely impacted by river damming (Skalska et al., 2020). Moreover, MPs involve a large range of particles sizes and densities and thus various transport capacities. While a high level of MP pollution in reservoir sediments has been established, our understanding of interactions between MP pollution and hydrosedimentary processes deserve to be improved. Dam reservoirs are structured according to dam functioning, hydraulic dynamics, bottom geomorphology, and sediment characteristics (Shotbolt et al., 2005; Skalak et al., 2013). Consequently, MP spatial distribution cannot be explained thoroughly by the source's influence alone (Di and Wang; 2018; Lin et al., 2021). The MP accumulation in sediments was explained by a fostering of the settling process in the water column, resulting from low-velocity and low-turbulent flow conditions (Lin et al., 2021; Kiss et al., 2021). Regarding the complexity of

depositional conditions in reservoirs, we need a more detailed view of the diversity of trapping processes for plastic particles in sediments. This issue is particularly relevant for the management of sediments retained in reservoirs, representing a challenge in many reservoirs worldwide (Hauer et al., 2018; Liu et al., 2018, Noe et al., 2020).

Knowledge of MP sedimentation and storage in engineered rivers remains a pending issue, including the processes governing MP deposition in river sediments (Waldschläger et al., 2022). In a riverine context, proportional relationships have been shown to exist between the MP content and the finest fractions of sediments (Enders et al., 2019; He et al., 2020). Laboratory experiments demonstrated a higher mobility of MPs when compared to same-sized sediment grains and an inaccuracy of the theoretical approaches for calculating their settling velocities (Waldschläger and Schüttrumpf, 2019ab). In the literature, several driving factors influencing the sinking/rising comportment of MPs are also reported, such as the size, density, shape and biofouling (Waldschläger and Schüttrumpf, 2020; van Melkebeke et al., 2020).

Dam reservoirs are good environments for improving our understanding of MP/sediment relationships, as they show great variations in terms of deposition processes, sediment transfer and water residence time. This paper focuses on the longitudinal evolution of MP levels in sediments of the Villerest reservoir– located in the upstream part of the Loire River basin, 36 km long - which is an optimal site because most MP potential sources are located about 50 km upstream of the reservoir inlet. The working hypothesis is that reservoirs, by deeply altering the river functioning and the sedimentation of transported materials, constitutes sinks for MP. In addition, as many reservoirs, it presents various depositional environments (e.g., riverine, transitional, and lacustrine-like zones) with contrasted hydrosedimentary processes. We postulate that the variability of the sedimentation conditions can largely control the spatial distribution of MP in sediments. The main aim of this work is to account for the context of MP contamination regarding:
(i) the geomorphic structure of the reservoir to localize eventual preferential contamination areas,
(ii) the hydrosedimentary processes specific to geomorphic structures
and (iii) the relationships with the composition of the sedimentary matrix, and to geomorphic structures.

The main novelty of this research is to investigate the role of reservoirs on the MP pollution distribution in sediments along river courses. Moreover, this work is based on an innovative approach combining MP analyses using µFTIR imaging (for a systematic characterization of MP ≥ 25 µm) and geomorphological and sedimentological analyses allowing to identify deposition processes from the sediment composition.

2. Materials and methods

2.1. Studied area and sampling strategy

The Villerest reservoir has a mean capacity of 138 Mm^3 over a controlled section of 36 km long. The dam's management allows a water level variation of 11 m over a year to control outflows during flood and low-water episodes and to produce hydropower energy. Since the dam operation in 1984, the outflow range has been regulated between 12 and 1,700 m^3/s.

According to the reservoir managers (EP-Loire), the thermic stratification of the reservoir, close to the dam, is well-established in July (depending on climate conditions), the thermocline being between 20 to 25 m deep. It is quite short-lived as in September, with the rapid cooling of the epilimnion and the hydraulic management of the reservoir, temperature of reservoir waters decreases, and the water column is thermally homogeneous by the end of December.

In the studied basin (6,607 km² basin, Fig. 1 ab), most of the potential MP sources are located upstream of the Villerest Reservoir at the distance of the reservoir tail (about 50 km of river course), as illustrated in Fig. 1b. To evaluate the distribution of these sources in the Villerest Dam basin, population density and wastewater treatment plant capacity were spatialised. The total population is 728 k inhabitants in the basin. Two areas are characteristic clustering industrial and urban areas of Saint-Étienne and Le Puy en Velay and their suburbs. The wastewater treatment capacity is 607 and 80 k population equivalent (p.e.) for these two areas respectively (for cumulative capacity of 979 k p.e. at the basin scale). The Grangent Dam Reservoir, located about 50 km upstream of the Villerest Dam, could constitute an important barrier for MPs coming from the most upstream part of the Loire basin.
The population and the wastewater treatment capacity present in the proximal catchment of the reservoir (*i.e.,* along the reservoir and its tributaries) only weigh 7% and 2% of the total Loire basin upstream of the Villerest Dam, respectively. This proximal catchment is mostly covered by extensive grazing and forest areas. Any industrial site producing or recycling plastic materials and dumping sites are referenced in this proximal catchment.

The sediment sampling campaign took place during June and July 2021, after the floods season and when the water level was between 314 and 315 m.a.s.l. (close to the maximum in anticipation of the water demand during the low-flow period). Depending on the water depth, a stainless-steel Ekman grab or a shovel with a telescopic rod was used to collect samples from a boat. Surface sediments were sampled over a depth of 15 cm maximum, by less than 1 m up to a depth of 35 m. After collection, the samples were stored in glass containers before analysis. Samples were collected every kilometre to study the geomorphic structure of sediment over a longitudinal profile integrating:

- 10 samples were collected from the section influenced by annual variation in the controlled water level (Sections A–B),
- 26 samples were from a section deep enough to always be under the controlled water level (Sections B–C),
- and three samples were taken downstream of the dam, up to the next major city (Roanne, Section C, Fig. 1c).

Once the reservoir structuration was done, MP analysis was performed on a more restricted number of subject samples.

2.2. Analytical method

Sedimentological analyses were performed on all sediment samples. Grain-size analyses were performed with a Malvern Mastersizer 3000 laser diffraction microgranulometer after a 30 s ultrasonic step (particle sizes ranged between 0.1 and 3,500 µm). Leaves and wood fragments present in some slices were manually removed before analysis. Grain-size statistics were calculated with the Gradistat program (Blott and Pye, 2001) using the geometric method of Folk and Ward. Total organic carbon (TOC) contents were measured in sediments after being sieved at 2 mm, crushed in an agate mortar and digested with orthophosphoric acid (3 times 1 ml, 1 M at 60°C over 24h until complete evaporation). Sample duplicates and reference samples (NIST SRM 2702) went under the same protocol. Analyses were carried using a Carbon-Sulfur Analyser (LECO-CS 844) with reference samples (NIST 2702, TOC ~3.27 wt%; SRM 1944, TOC = 4.4±0.3 wt%) run at the same time every 10 samples. Reproducibility was better than 5%, and accuracy was within 5% of the certified values.

For MP analysis, 21 samples from 39 total were selected across the reservoir and downstream according to the geomorphic structures (defined later in § 3.1). Seven sampling points (one in each geomorphic structure) were analysed in triplicate to evaluate the reproducibility of the analytical process. To reduce any bias due to the heterogeneity of the samples, about 15–40 g of homogenized

wet sediments were subsampled to obtain 10 g of dry mass. To avoid cross-contamination during the drying step, the water content was determined independently from another subsample (after 24 h at 105 °C).

A three-step extraction protocol was performed to isolate MPs from sediments, following the current best practice (Nakajima et al., 2019; Phuong et al., 2021, SM. 1):

i. Organic matter was eliminated from bulk sediments via hydrogen-peroxide digestion (H_2O_2 30% – Fluka Germany – at 45 °C, for 24 h with slow agitation). The solid phase was then recovered using a metallic filter (10 µm cutoff).

ii. According to the protocol proposed by Nakajima et al. (2019), density separation was then performed over 24 h with an iodide sodium solution (NaI – VWR, with a density > 1.6 $g.cm^{-3}$). Thereafter, the supernatant was filtered with a metallic filter to recover the low-density solid phase.

iii. A second hydrogen-peroxide digestion step was performed on the supernatant to remove the residual natural organic matter. MPs were then set on Anodisc (Whatman) membrane filters (0.2 µm, 25 mm) by filtration. The final filter was dried at room temperature and conserved in a glass petri dish until analysis.

Plastic particles were analysed by µFTIR imaging (micro-Fourier Transform InfraRed; Thermo Nicolet iZ10). A pixel with a resolution of 25 µm was selected; hence, previous filtration steps did not influence the counting of the MPs. µFTIR imaging was performed for the entire sample (*i.e.,* the entire filtration zone of the sample) and not only with subsampling (as was traditionally done in previous studies).

Acquisition parameters were described in a recent study (Treilles et al., 2021). The µFTIR maps were treated with siMPle software (v.1.1.β, Primpke et al., 2018) and the library MP_Library_extended_grouped_1_5.txt. The default matching weight of 0.5 for the first derivative of the spectra and 0.5 for the second derivative of the spectra was used, and the AAU pipeline was chosen for data processing. Based on a 25 µm resolution, the minimal particle size provided by siMPle is 32 µm. The largest plastic sizes provided in the output of the siMPle software were considered.

2.3. Microplastic quality analysis and quality control

Contamination prevention was strictly respected at all stages of the procedure. Plastic equipment was prohibited during the whole field sampling and laboratory protocols. Before utilization, the laboratory equipment was rinsed three times with ultrapure water (Progard® TS2). All solutions were prepared and filtered on a glass fibre filter (0.7 µm, Fisher Scientific) and then utilized in a short time. Clean working conditions were maintained using a closed fume hood (Labo Pratic, France) prewashed with ethanol, cotton lab coats and nitrile gloves for lab technicians and aluminium foil to protect the samples.

Quality control was also monitored. Lab airborne deposition, ultrapure water and material contamination were tested *via* a blank protocol. Lab blanks were performed (n = 3). No MP was identified in the blanks except for one polyethylene (PE) particle, attesting to the control of laboratory work contamination.

3. Results

3.1. Geomorphic structures and associated hydrosedimentary processes

In the Villerest Reservoir, the water level varies between 312 and 315.3 m.a.s.l. over the hydrological year (Fig. 2). It can be downramped to 304 m.a.s.l. only to prevent important flood episodes for a few

weeks in a year. Hence, the reservoir can be divided into an upstream segment of 4 km long that is frequently subjected to hydrofluctuations (kilometre point, KP, 0–4), a 7 km segment that is occasionally dewatered (KP 5–11, composed of the A-B section in Fig. 1) and a 26 km long segment always under its influence (KP 12–36, the B-C section). The reservoir topography marks a transition after KP 4 from a relatively flat segment (0.2 ‰) to a steeper slope (1.7 ‰) of the river bottom. Between KP 9 and 30, the slope becomes gentler (1.1 ‰). The last 6 km of the reservoir constitutes the deepest area (> 30 m deep). The bottomset is flatter, especially over the last 3 km of the reservoir. Downstream from the Villerest Dam, the channel slope is 0.5 ‰.

Two sediment typologies can be recognized in this study area:

- The first group corresponds to coarse-grained sediments (CGS) with a median grain size (D_{50}) ranging between 808 and 1,320 µm (Fig. 2). It is mostly composed of well-sorted coarse to very coarse sands (86.7–98.6%). Very fine gravels were slightly present (1.1–4.9%). Silts only weighed a low percentage (not detected to 9.6%). A low TOC content also characterized these deposits (0.1–0.6%). This sediment group is located in the most upstream part of the reservoir (KP 0–8) and just downstream of the dam. Two samples are finer: at KP 6 (upstream of the confluence with the Aix River; D_{50} = 43 µm) and at KP 38 km (D_{50} = 247 µm), as the sample was recovered in the riverbank (not possible to sample the riverbed at this station).

- The second group is much finer, with a D_{50} ranging between 15 and 93 µm (Fig. 2). It is mostly composed of fine-grained sediments (FGS, 42.3–89.7%) and is poorly sorted. Clays are present in a low proportion (0.2–1.3%). The TOC content is significantly higher than that of the first group, ranging between 1.7 and 4.9%. These deposits are present over a 28 km long segment (from KP 9 to the dam). Specifically, at KP 13, sediment is richer in sands and poorer in TOC related to a punctual channel narrowing of the Loire River.

Based on these results, geomorphic structures related to the dam's presence and associated with its operations can be identified (Fig. 2). The river section from KP 0 to 11 corresponds to a reservoir-dominated transitional reach and the riverine zone. The CGS forms a long delta that can be divided into a relatively flat delta topset (up to KP 4) and a steeper delta foreset (KP 5–8) under the influence of frequent hydrofluctuations. A margin is present at the front of this delta (KP 8–11). More frequently dewatered deposits are also richer in FGS and TOC. The final transition to the reservoir reach (KP 12–36) is always under the dam's influence. For the next 13 km, a transitional zone is present where lacustrine-like sedimentation dominates (poorly sorted silts and clays), even if riverine sedimentation (coarser load composed of well-sorted sands) exerts an influence (KP 12–24). Downstream of this limit (KP 25–36), only lacustrine-like sedimentation contributes. These two structures are named Bottomsets 1 and 2 in Fig. 2. A muddy lake can be identified over the last 3 km with an important accumulation of sediment adjusting the natural topography. Downstream from the dam, an important lack of sediments is reported, suggesting a severe armouring of the channel in this reach.

Regarding grain size distributions and their deconvolutions (SM.2), riverine, transitional and lacustrine-like sedimentations can be related with specific hydrosedimentary processes. In the riverine zone (delta and downstream of the dam), CGS essentially originate from a bed load transport mobilized during flood events. In the transitional zone (margin and Bottomset 1), the coarsest fraction of sediments is also essentially transported during flood events as turbidity underflows. FGS are transported in suspension, accumulate in the controlled section before a long-time settling process because of low-velocity and low-turbulent flow conditions. When conditions are favorable to the settling process, FGS can also temporally deposit in the riverine zone, but they are winnowed during hydrologic events or/and when the water level change.

3.2. Microplastic levels in sediments

The MP content was analysed in the seven defined geomorphic structures (Fig. 3), and 21 samples were analysed, with 2–7 samples per geomorphic structure. Triplicates were performed for each sample, bringing the total amount of analyses to 35.

Two different groups were defined according to MP abundance (Kruskal–Wallis test, p value < 0.05, n = 35):

- The first gathers riverine zones (the delta and downstream of the dam). Sediment contamination ranges between 0.9 and 1.6 10^3 items/kg dw (minimum of 0.4 – maximum of 7.8 10^3 items/kg dw). For this group, the median content is 1.4 10^3 items/kg dw, and the 25% and 75% percentiles are 1.2 and 1.5 10^3 items/kg dw (n = 12).

- The second is composed of transitional and lacustrine-like zones (the margin, bottomsets and the muddy lake). The median MP content ranged between 0.7 and 1.3 10^4 items/kg dw (0.3–3.0 10^4 items/kg dw). The MP level is much higher than that in the first group, with a median content of 1.1 10^4 items/kg dw, and 0.6 and 1.4 10^4 items/kg dw, for the 25% and 75% percentiles, respectively (n = 23).

Regarding the MP content, these two groups matched the distinction between CGS and FGS. A sharp increase in the MP content by one order of magnitude occurs in the reservoir in relation to a change in the sedimentation process leading to settling of the fraction < 63 µm.

Triplicates were analysed in each geomorphic structure to compare intrasample to intersample statistical spread. Triplicate variance accounted for less than 1% of the total variance in the CGS (n = 9), but it reached 79% in the FGS (n = 12). This attests to a good counting reproducibility in CGS, rather than the dispersion being much larger in FGS. Due to the high variance observed in FGS, the spatial analysis was performed by comparing geomorphic structures, each one with triplicates.

3.3. Polymer diversity

Regarding all samples, polypropylene (PP) and polyethylene (PE) particles represent 88% of the 2,346 MPs pinpointed with the µFTIR imaging (SM.3). With polystyrene (PS), they account for 95% of typified MPs. The remaining 5% are polyurethane (PU), polyvinylchloride (PVC), polyester, polyamide (PA) and to a lesser extent (less than 1%), subcomponents of the polyester family such as alkyd, acrylic, polyvinyl acetate (PVAC) and copolymers such as acrylonitrile butadiene styrene (ABS) and cellulose acetate.

In detail, based on the 34–874 items detected in each geomorphic structure, the two dominant polymers (PP and PE) range in balanced proportions between 30% and 60% in each unit (Fig. 4). The PS counts for less than 2% in CGS of the delta and downstream of the dam, whereas this polymer is present in a higher proportion in the FGS section of the reservoir (4–12%). This trend is also observed for other polymers. While they are very poorly detected in the CGS (often absent, 1–3 items by unit), they are more regularly identified in the FGS. Here, they still represent a low proportion of total MP (up to 3%), but a dozen items by units were identified for PU, PVC or PA (11–13 items), while fewer items were identified for alkyd, polyester, ABS, and acrylic (4–6 items). Even in FGS, cellulose acetate and PVAC are very rarely detected (1 item by unit).

In all geomorphic structures, pp, pe and in a lesser extent ps are majority polymers. Minority polymers (those counting for less than 5 % of typified MPs) are more diversified in geomorphic structures with FGS (between 5 and 7 additional polymers) than in those with CGS (between 1 and 3 additional polymers).

Over the FGS section, the three predominant polymers show different evolutions. The PP presents stable levels from the margin to the muddy lake (KP 9–36), with median contents of 3.9 10^3 and 3.7 10^3 items/kg dw. However, the two other polymers decrease over this section from a median content of 6.0 10^3–2.5 10^3 items/kg dw for PE and from 1.5 10^3–0.5 10^3 items/kg dw for PS, corresponding to reductions of 58% and 65%, respectively.

These results attest to an evolution of the polymer mixture in sediments depending on the presence of FGS and to a partition operating during transport through the reservoir.

3.4. Microplastic particle size

The minimum MP size measured was 32 µm, and the maximum was 3,328 µm (Fig. 5). The median particle size was restrained in a relatively narrow range between 110 and 177 µm in each geomorphic structure. The percentiles of 25% and 75% lie between 81 and 343 µm. Regarding all samples, the median particle size was 137 µm (percentiles 25% and 75% equal to 96 and 252 µm, respectively).

For PP and PS, the median ranged between 81 and 177 µm, whereas it was slightly higher for PE (between 171 and 302 µm). For other polymers, the median particle sizes are on the same order of magnitude (60–427 µm), except for the alkyd, which is sensibly coarser (243–1,228 µm).

The MP size distribution is relatively similar between geomorphic structures compared with sediment grain-size variations.

4. Discussion

4.1. Microplastic trapping in dam reservoirs

Substantial MP levels are emphasized in sediments of the Villerest Reservoir (order of 10^4 items/kg over a 28 km long section). MP contents obtained in this study are much higher than those previously reported in other reservoirs, partly due to the larger target size range (*i.e.,* ≥ 32 µm whereas the detection size limit varies between 90 and 200 µm in selected studies, SM. 4). Based on these higher size limits, MP levels would range 13 and 64% less respectively for CGS maximum, 20 and 57% less for FGS maximum. However, even with same size limits MP levels in FGS of the Villerest reservoir are about one order of magnitude higher than in selected studies of SM. 4. µFTIR imaging is rarely used, and the novelty was here to perform a 25 µm resolution and mapping over the entire sample. Additionally, most selected studies use visual identification under a microscope before the identification of isolated particles. This step limits the performance of this method for particles smaller than 100 µm (Primpke et al., 2020). In the Villerest Reservoir, about 50% of the identified MPs range between 32 and 100 µm.

The Loire valley upstream of the reservoir drains an important industrial and urban area at the national scale around the Saint-Étienne agglomeration (§ 2.1). Wastewater effluents and sludge, as well as runoff of contaminated industrial and urban surfaces, are considered in the literature as major sources for MPs in river systems (e.g., Dris et al., 2018; Schmidt et al., 2020, Waldschläger et al., 2020). Moreover, this contamination hotspot includes many plastic industries, essentially producing packaging and automotive plastics. Even if these potentially significant MP sources are far away (about 50 km of the river course), severe contamination affects FGS trapped in the reservoir. In addition, the Loire River morphology between the contamination hotspot and the Villerest Reservoir is mainly a straight and steep channel running in a partly confined valley. In these geomorphological conditions, the river velocity is relatively high, providing favorable conditions for the long-distance transport of MPs (He et al., 2021). Thus, the Villerest Reservoir creates an accumulation environment for sediments and MPs along the Loire River course.

A strong influence of the Villerest Reservoir is highlighted on the longitudinal evolution of sedimentary MP contaminations in the upper part of the Loire River, which are locally amplified by favorable settling conditions. River fragmentation by human-induced barriers, including large damming, is very widespread worldwide (Lehner et al., 2011; Grill et al. 2019, Belletti et al., 2020). Under these conditions, the accumulation of FGS in reservoirs can have a large influence on the transport of MPs to the global oceans.

4.2. Sediment composition as a proxy of favorable conditions for microplastic trapping

A non-size-controlled sedimentation for plastic particles is highlighted in CGS and in FGS over the range size analysed (32–3,328 µm). In addition, the polymer abundance does not present any direct correlation with the sediment composition in terms of grain-size and TOC content (Pearson correlation, r positive, $p < 0.05$, $n = 35$, Table 1). Here, it can be considered a step increase in the MP content with the presence, in a significant proportion, of FGS richer in TOC. From an empirical point of view, the presence of silts and clays is related to hydrological conditions fostering the sedimentation of the finest particles and preventing them from reworking (low-velocity and low-turbulent flow). The stronger TOC content usually measured in such FGS is also a manifestation of these conditions leading to the settling and archiving of low-density particles such as MPs. Moreover, in the delta, the TOC can largely be associated with vegetal macrorests (generally > 2 mm) deposited with sands during floods.

The presence of FGS in transitional and lacustrine-like zone is an indicator of the settling process and leads to an increase in the MP content and polymer diversity. The relatively homogenous MP size pattern over the section dominated by fine-grained sedimentation can be related to the poor grain-size sorting of FGS. The relatively heterogeneous grain-size distribution indicates a low size-partition process for particles settling in the water column. Moreover, in such a reservoir context, there are complementary factors that foster MP sedimentation, such as aggregation with suspended sediments, natural organic matter, or biofouling (*e.g.*, Besseling et al., 2017; Li et al., 2019; Leiser et al., 2020, 2021; Halsband, 2021).

In the riverine zone with CGS, different mechanisms can explain the presence of MPs in the bed load (Skalska et al., 2020). MP infiltration, *i.e.,* diffusion/transfer, into the CGS porosity is a relevant process to explain our observations (Frei et al., 2019; Waldschlager and Schüttrumpf, 2020) and is complementary to the adverse balance between sedimentation and resuspension described above.

These transport/deposition mechanisms can explain the difference of MP contents and polymer compositions between CGS and FGS. In addition, while CGS mostly give access to MPs instantly transported or temporary intercepted in the sediment porosity, the MP mixture settling with FGS is representative of a longer time inflow, including various hydrological conditions. The Villerest reservoir is notably used to regulate the Loire River flow during these events. Floods are known to mobilized higher MP concentrations and modified the composition of the polymer mixture, because of specific sources activations (Hitchcock, 2020; de Carvalho et al., 2022). The similarity of the range of MP sizes between CGS and FGS could highlight a stable size signature of the MP load provided by the Loire River. Another hypothesis would be that hydrosedimentary process variations do not significantly influence MP size.

Finally, the integrated approach combining MP, geomorphological and sedimentological analysis is a suitable way to study the fate of MP contaminations in sedimentary deposits subjected to complex hydrosedimentary processes.

4.3. Evidence of a density-controlled partition of polymers

In riverine environments, polymer sorting can occur in sediments as a function of their density and stream shear stress (Enders et al., 2019). In a reservoir, sedimentation is principally driven by settling processes, and the spread of MP contamination first occurs by diffusion/accumulation in the water body. Under low-flow velocity conditions, a vertical partition of polymers can appear, controlled by particle density, as suggested by Lenaker et al. (2019).

A partition of the dominant polymers was observed along the Villerest reservoir in transitional and lacustrine-like zones. While the PP level remained constant in FGS, the content of PE and PS significantly decreased from the margin to the dam. The three polymers have distinct relative density ranges: PP = 0.83–0.87, PE = 0.94–0.98, and PS = 1.01–1.02 (Waldschläger and Schüttrumpf, 2019a). Our hypothesis is that polymers with the highest densities (PE, PS) progressively dwindle in the water column along the longitudinal gradient in the reservoir. This process could be amplified by the increasing water depth, leading to an ever longer settling time to reach the reservoir bottom. Particles of PP, which are less dense than PE and PS particles, could have a delayed sinking mechanism, which can explain the constant polymer deposit over the section.

The conceptual design of the inflow spread in a reservoir can involve stratified currents according to the density difference in the water column. Moreover, the existence of plunge points has been shown where the flow density equals the surrounding water, entrapping particles at the bottom (Yu et al., 2000). The thermic stratification of the reservoir may influence this process. Such a stratification seasonally occurs in the Villerest reservoir (§ 2.1). When applied to MPs, this process can explain the density-controlled polymer partition observed in the sediments. It also matches other observations of partitions in the water column in other reservoirs (Lin et al., 2021).

5. Environmental implications

We found a clear link between the reservoir structuring, sediment composition and MP levels. MPs preferentially accumulate with FGS in sections under a controlled water level. In the upper part of reservoirs (*i.e.,* in the delta with CGS), conditions are less favorable for MP trapping because of an adverse balance between sedimentation and resuspension processes in relation to higher flow velocity and turbulence. Additionally, it constitutes the hydrofluctuation belt subjected to alternating steps of MP deposits and remobilization (Zhang et al., 2019).

By accumulating and fostering the MPs settling important levels can be reached in reservoir, even at substantial distances from sources. Sediment accumulation raises the issue of sustainability for many reservoirs, requiring management operations in certain circumstances (Kondolf et al., 2014; Schleiss et al., 2016; Hauer et al., 2018). Hence, MPs can be massively resuspended in the water column during sediment erosion/dredging works, and they could be more easily mobilizable than the mineral fraction of sediments (Enders et al., 2019; Waldschläger and Schüttrumpf, 2019ab).

Our findings provide significant elements for a better consideration of MP pollution in sediment management (at least downstream of substantial sources). Presently, contamination risks for downstream sections were weakly evaluated, even if important MP release can be expected during management operations (Song et al., 2020). River restoration programs such as dam removal can then lead to a substantial release of FGS retained by infrastructures, and thus the potentially associated MPs.

6. Conclusion

To better understand the microplastic trapping process in dam reservoirs, we combined geomorphological, sedimentological and microplastics analyses in a dam reservoir context to study the longitudinal evolution of the microplastic content. The Villerest Reservoir is a particularly appropriate study case, as it is located far away from substantial microplastic sources. Under these conditions, microplastic variations were mainly related to sedimentation processes in reservoirs.

A higher microplastic level and diversity is highlighted in fine-grained deposits of transitional and lacustrine-like zones compared with coarser sediments of the riverine zones (by one order of magnitude). Preferential MP deposits are associated with fine-grained sedimentation under regular hydrofluctuation levels. Such findings specify the microplastic pollution in reservoir sediments. They also provide insight for a better consideration of microplastic pollution during sediment management.

Non-size-controlled sedimentation is reported for microplastics, and the polymer abundance is not directly correlated with sediment composition (grain size, carbon parameters). Under these conditions, the microplastic pollution in coarse-grained sediments corresponds to a weak capture of the flow transported by the Loire River, and a larger part settles with fine-grained sediments. A density-controlled partition of polymers is illustrated over the transitional and lacustrine-like zones, certainly related to a flow stratification process typical in reservoirs.

An important microplastic trapping with fine-grained sediments is demonstrated. Infrastructure-induced conditions fostering the settling of fine-grained sediments are very widespread in regulated rivers. They concern not only reservoirs in the riverbed but also in floodplains along overbanks. This suggests the existence of important microplastic stocks with fine-grained deposits. It also encourages continued research concerning microplastic pollution in sediments and supports a specific focus on fine-grained sediments in depositional environments.

Declaration of competing interest:

The authors declare that they have no known competing monetary interests or personal relationships that could have influenced the work reported in this paper.

CRediT authorship contribution statement:

Elie Dhivert: Conceptualization, Sampling, Analyses, Data processing and investigation, Writing - Original Draft, Visualization. **Ngoc-Nam Phuong**: Conceptualization, Analyses, Validation, Investigation, Writing - Review & Editing**. Brice Mourier**: Conceptualization, Sampling, Investigation, Writing - Review & Editing, Supervision. **Cecile Grosbois**: Conceptualization, Sampling, Investigation, Writing - Review & Editing, Supervision. **Johnny Gasperi**: Conceptualization, Sampling, Investigation, Writing - Review & Editing, Supervision, Project administration, Funding acquisition.

Acknowledgements:

This study was carried out both in the framework of the Sedi-Plast research program funded by the French Research Agency (ANR-19-CE34-0012) and the Plasti-nium research project funded by Nantes Métropole and Pays de la Loire Region.

7. References

Belletti, B., Garcia de Leaniz, C., Jones, J., Bizzi, S., Börger, L., Segura, G., ... & Zalewski, M. (2020). More than one million barriers fragment Europe's rivers. Nature, 588(7838), 436-441.

Bertrand, O., Mondamert, L., Grosbois, C., Dhivert, E., Bourrain, X., Labanowski, J., & Desmet, M. (2015). Storage and source of polycyclic aromatic hydrocarbons in sediments downstream of a major coal district in France. Environmental pollution, 207, 329-340.

Besseling, E., Quik, J. T., Sun, M., & Koelmans, A. A. (2017). Fate of nano-and microplastic in freshwater systems: A modeling study. Environmental pollution, 220, 540-548.

Blott, S. J., & Pye, K. (2001). GRADISTAT: a grain size distribution and statistics package for the analysis of unconsolidated sediments. Earth surface processes and Landforms, 26(11), 1237-1248.

Culicov, O. A., Trtić-Petrović, T., Balvanović, R., Petković, A., & Ražić, S. (2021). Spatial distribution of multielements including lanthanides in sediments of Iron Gate I Reservoir in the Danube River. Environmental Science and Pollution Research, 28(33), 44877-44889.

de Carvalho, A. R., Riem-Galliano, L., Ter Halle, A., & Cucherousset, J. (2022). Interactive effect of urbanization and flood in modulating microplastic pollution in rivers. Environmental Pollution, 309, 119760.

Di, M., & Wang, J. (2018). Microplastics in surface waters and sediments of the Three Gorges Reservoir, China. Science of the Total Environment, 616, 1620-1627.

Dris, R., Imhof, H., Sanchez, W., Gasperi, J., Galgani, F., Tassin, B., & Laforsch, C. (2015). Beyond the ocean: contamination of freshwater ecosystems with (micro-) plastic particles. *Environmental chemistry*, *12*(5), 539-550.

Enders, K., Käppler, A., Biniasch, O., Feldens, P., Stollberg, N., Lange, X., ... & Labrenz, M. (2019). Tracing microplastics in aquatic environments based on sediment analogies. Scientific reports, 9(1), 1-15.

Frei, S., Piehl, S., Gilfedder, B. S., Löder, M. G. J., Krutzke, J., Wilhelm, L., & Laforsch, C. (2019). Occurence of microplastics in the hyporheic zone of rivers. Scientific reports, 9(1), 1-11.

Grill, G., Lehner, B., Thieme, M., Geenen, B., Tickner, D., Antonelli, F., ... & Zarfl, C. (2019). Mapping the world's free-flowing rivers. Nature, 569(7755), 215-221.

Guo, Z., Boeing, W. J., Xu, Y., Borgomeo, E., Mason, S. A., & Zhu, Y. G. (2021). Global meta-analysis of microplastic contamination in reservoirs with a novel framework. Water Research, 207

Halsband, C. (2021). Effects of Biofouling on the Sinking Behavior of Microplastics in Aquatic Environments. In Handbook of Microplastics in the Environment (pp. 1-13). Cham: Springer International Publishing.

Hauer, C., Wagner, B., Aigner, J., Holzapfel, P., Flödl, P., Liedermann, M., ... & Habersack, H. (2018). State of the art, shortcomings and future challenges for a sustainable sediment management in hydropower: A review. Renewable and Sustainable Energy Reviews, 98, 40-55.

He, B., Smith, M., Egodawatta, P., Ayoko, G. A., Rintoul, L., & Goonetilleke, A. (2021). Dispersal and transport of microplastics in river sediments. Environmental pollution, 279, 116884.

He, B., Wijesiri, B., Ayoko, G. A., Egodawatta, P., Rintoul, L., & Goonetilleke, A. (2020). Influential factors on microplastics occurrence in river sediments. Science of the Total Environment, 738, 139901.

Hitchcock, J. N. (2020). Storm events as key moments of microplastic contamination in aquatic ecosystems. Science of the Total Environment, 734, 139436.

Kiss, T., Fórián, S., Szatmári, G., & Sipos, G. (2021). Spatial distribution of microplastics in the fluvial sediments of a transboundary river–A case study of the Tisza River in Central Europe. Science of the Total Environment, 785, 147306.

Kondolf, G. M., Gao, Y., Annandale, G. W., Morris, G. L., Jiang, E., Zhang, J., ... & Yang, C. T. (2014). Sustainable sediment management in reservoirs and regulated rivers: Experiences from five continents. Earth's Future, 2(5), 256-280.

Lehner, B., Liermann, C. R., Revenga, C., Vörösmarty, C., Fekete, B., Crouzet, P., ... & Wisser, D. (2011). High-resolution mapping of the world's reservoirs and dams for sustainable river-flow management. Frontiers in Ecology and the Environment, 9(9), 494-502.

Leiser, R., Jongsma, R., Bakenhus, I., Möckel, R., Philipp, B., Neu, T. R., & Wendt-Potthoff, K. (2021). Interaction of cyanobacteria with calcium facilitates the sedimentation of microplastics in a eutrophic reservoir. Water Research, 189, 116582.

Leiser, R., Wu, G. M., Neu, T. R., & Wendt-Potthoff, K. (2020). Biofouling, metal sorption and aggregation are related to sinking of microplastics in a stratified reservoir. Water research, 176, 115748.

Lenaker, P. L., Baldwin, A. K., Corsi, S. R., Mason, S. A., Reneau, P. C., & Scott, J. W. (2019). Vertical distribution of microplastics in the water column and surficial sediment from the Milwaukee River Basin to Lake Michigan. Environmental science & technology, 53(21), 12227-12237.

Li, Y., Wang, X., Fu, W., Xia, X., Liu, C., Min, J., ... & Crittenden, J. C. (2019). Interactions between nano/micro plastics and suspended sediment in water: Implications on aggregation and settling. Water research, 161, 486-495.

Lin, L., Pan, X., Zhang, S., Li, D., Zhai, W., Wang, Z., ... & Crittenden, J. C. (2021). Distribution and source of microplastics in China's second largest reservoir-Danjiangkou Reservoir. Journal of Environmental Sciences, 102, 74-84.

Liu, C., Walling, D. E., & He, Y. (2018). The International Sediment Initiative case studies of sediment problems in river basins and their management. International Journal of Sediment Research, 33(2), 216-219.

Nakajima, R., Tsuchiya, M., Lindsay, D. J., Kitahashi, T., Fujikura, K., & Fukushima, T. (2019). A new small device made of glass for separating microplastics from marine and freshwater sediments. PeerJ, 7, e7915.

Noe, G. B., Cashman, M. J., Skalak, K., Gellis, A., Hopkins, K. G., Moyer, D., ... & Hupp, C. (2020). Sediment dynamics and implications for management: state of the science from long-term research in the Chesapeake Bay watershed, USA. Wiley Interdisciplinary Reviews: Water, 7(4), e1454.

Phuong, N. N., Duong, T. T., Le, T. P. Q., Hoang, T. K., Ngo, H. M., Phuong, N. A., ... & Sempere, R. (2021). Microplastics in Asian freshwater ecosystems: Current knowledge and perspectives. Science of The Total Environment, 151989.

Primpke, S., Wirth, M., Lorenz, C., & Gerdts, G. (2018). Reference database design for the automated analysis of microplastic samples based on Fourier transform infrared (FTIR) spectroscopy. Analytical and bioanalytical chemistry, 410(21), 5131-5141.

Primpke, S., Christiansen, S. H., Cowger, W., De Frond, H., Deshpande, A., Fischer, M., ... & Wiggin, K. J. (2020). Critical assessment of analytical methods for the harmonized and cost-efficient analysis of microplastics. Applied Spectroscopy, 74(9), 1012-1047.

Rapin, A., Rabiet, M., Mourier, B., Grybos, M., & Deluchat, V. (2020). Sedimentary phosphorus accumulation and distribution in the continuum of three cascade dams (Creuse River, France). Environmental Science and Pollution Research, 27(6), 6526-6539.

Schleiss, A. J., Franca, M. J., Juez, C., & De Cesare, G. (2016). Reservoir sedimentation. Journal of Hydraulic Research, 54(6), 595-614.

Schmidt, C., Kumar, R., Yang, S., & Büttner, O. (2020). Microplastic particle emission from wastewater treatment plant effluents into river networks in Germany: loads, spatial patterns of concentrations and potential toxicity. *Science of the Total Environment*, *737*, 139544.

Shotbolt, L. A., Thomas, A. D., & Hutchinson, S. M. (2005). The use of reservoir sediments as environmental archives of catchment inputs and atmospheric pollution. Progress in physical geography, 29(3), 337-361.

Skalak, K. J., Benthem, A. J., Schenk, E. R., Hupp, C. R., Galloway, J. M., Nustad, R. A., & Wiche, G. J. (2013). Large dams and alluvial rivers in the Anthropocene: The impacts of the Garrison and Oahe Dams on the Upper Missouri River. Anthropocene, 2, 51-64.

Skalska, K., Ockelford, A., Ebdon, J. E., & Cundy, A. B. (2020). Riverine microplastics: Behaviour, spatio-temporal variability, and recommendations for standardised sampling and monitoring. Journal of Water Process Engineering, 38, 101600.

Song, J., Hou, C., Zhou, Y., Liu, Q., Wu, X., Wang, Y., & Yi, Y. (2020). The flowing of microplastics was accelerated under the influence of artificial flood generated by hydropower station. Journal of Cleaner Production, 255, 120174.

Treilles, R., Gasperi, J., Gallard, A., Saad, M., Dris, R., Partibane, C., ... & Tassin, B. (2021). Microplastics and microfibers in urban runoff from a suburban catchment of Greater Paris. Environmental Pollution, 287, 117352.

van Emmerik, T., Mellink, Y., Hauk, R., Waldschläger, K., & Schreyers, L. (2022). Rivers as plastic reservoirs. Front. Water, 3, 1-8.

Van Melkebeke, M., Janssen, C., & De Meester, S. (2020). Characteristics and sinking behavior of typical microplastics including the potential effect of biofouling: implications for remediation. Environmental science & technology, 54(14), 8668-8680.

Waldschläger, K. L., & Schüttrumpf, H. (2019a). Effects of particle properties on the settling and rising velocities of microplastics in freshwater under laboratory conditions. Environmental science & technology, 53(4), 1958-1966.

Waldschläger, K., & Schüttrumpf, H. (2019b). Erosion behavior of different microplastic particles in comparison to natural sediments. Environmental science & technology, 53(22), 13219-13227.

Waldschläger, K., & Schüttrumpf, H. (2020). Infiltration behavior of microplastic particles with different densities, sizes, and shapes—from glass spheres to natural sediments. Environmental Science & Technology, 54(15), 9366-9373.

Waldschläger, K., Brückner, M. Z., Almroth, B. C., Hackney, C. R., Adyel, T. M., Alimi, S. O., ... & Wu, N. (2022). Learning from natural sediments to tackle microplastics challenges: A multidisciplinary perspective. Earth-Science Reviews, 104021.

Waldschläger, K., Lechthaler, S., Stauch, G., & Schüttrumpf, H. (2020). The way of microplastic through the environment–Application of the source-pathway-receptor model. Science of the Total Environment, 713, 136584.

Watkins, L., McGrattan, S., Sullivan, P. J., & Walter, M. T. (2019). The effect of dams on river transport of microplastic pollution. Science of the Total Environment, 664, 834-840.

Wu, F., Wang, J., Jiang, S., Zeng, H., Wu, Q., Chen, Q., & Chen, J. (2022). Effect of cascade damming on microplastics transport in rivers: A large-scale investigation in Wujiang River, Southwest China. Chemosphere, 134455.

Yu, W. S., Lee, H. Y., & Hsu, S. M. (2000). Experiments on deposition behavior of fine sediment in a reservoir. Journal of Hydraulic Engineering, 126(12), 912-920.

Zhang, K., Chen, X., Xiong, X., Ruan, Y., Zhou, H., Wu, C., & Lam, P. K. (2019). The hydro-fluctuation belt of the Three Gorges Reservoir: Source or sink of microplastics in the water?. Environmental Pollution, 248, 279-285.

Figures and tables:

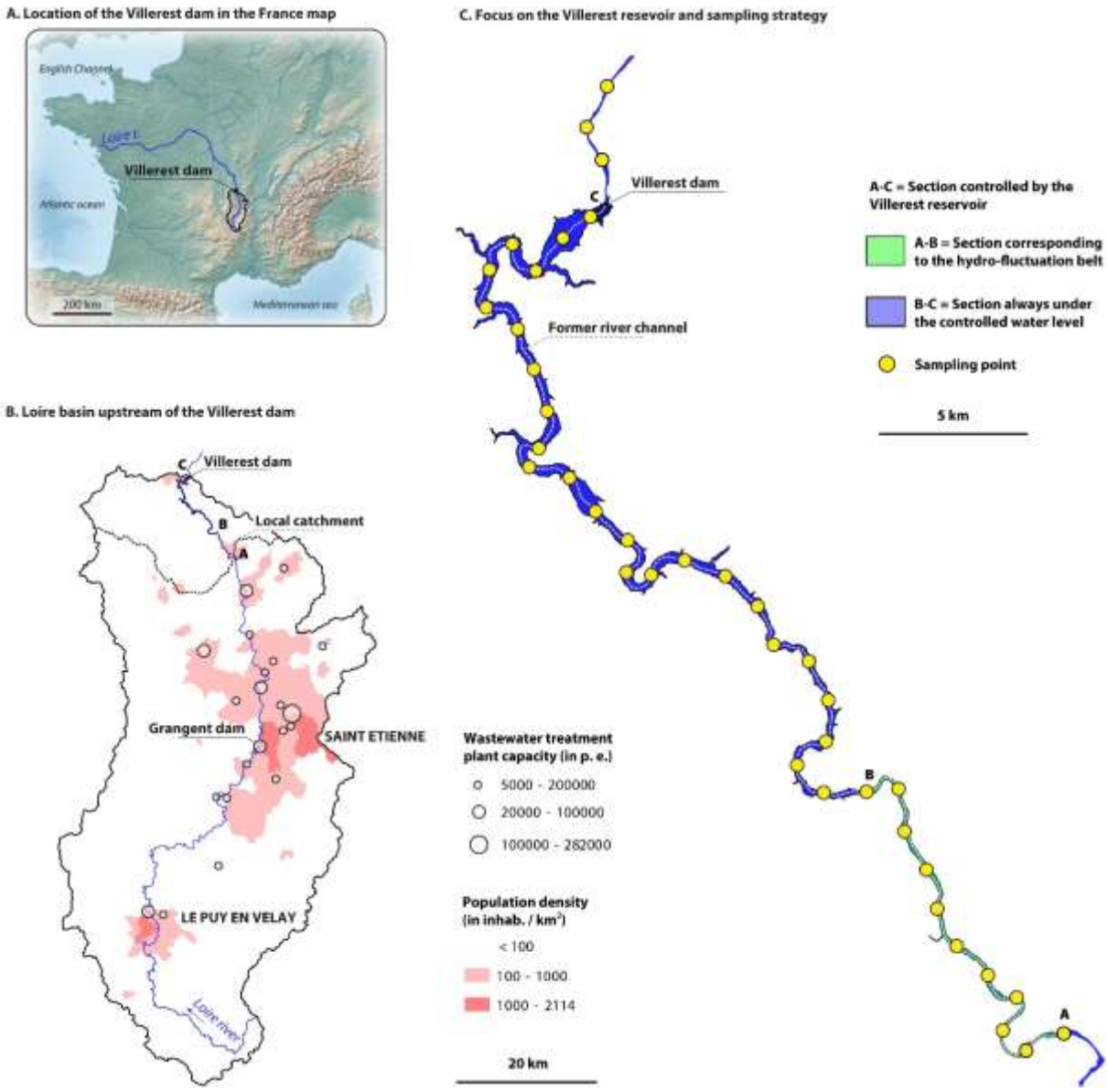

Fig. 1: A – Location of the Villerest Dam and its upstream basin in the Western Europe map (source: www.copernicus.eu); B – The Loire River basin upstream of the Villerest Dam (solid line) and the proximal basin of the reservoir (dotted lines), associated with the population density calculated at the France scale (source: www.insee.fr) and wastewater treatment plant capacities (source: www.sandre.eaufrance.fr); C – Focus on the controlled river section of the Villerest Reservoir and the sediment sampling strategy (in white and dotted line the former channel of the Loire River).

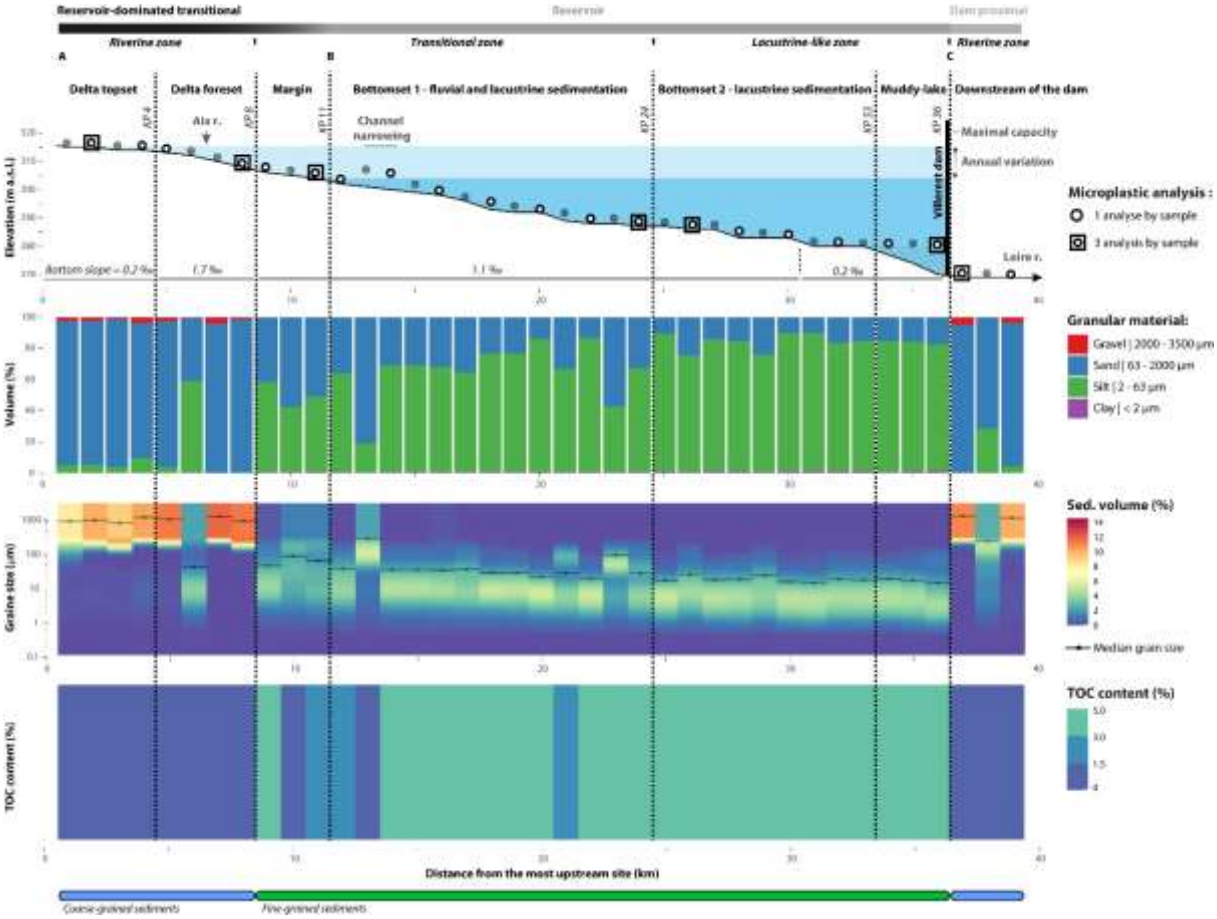

Fig. 2: Geomorphic structuring of the Villerest Reservoir according to the elevation profile, water level variation and sediment characteristics. The sedimentological characterization considers longitudinal evolutions of (i) granular materials, (ii) grain size distributions and (iii) total organic carbon (TOC) contents, all analysed in bulk sediments. Samples used for microplastic analyses are also shown with white points.

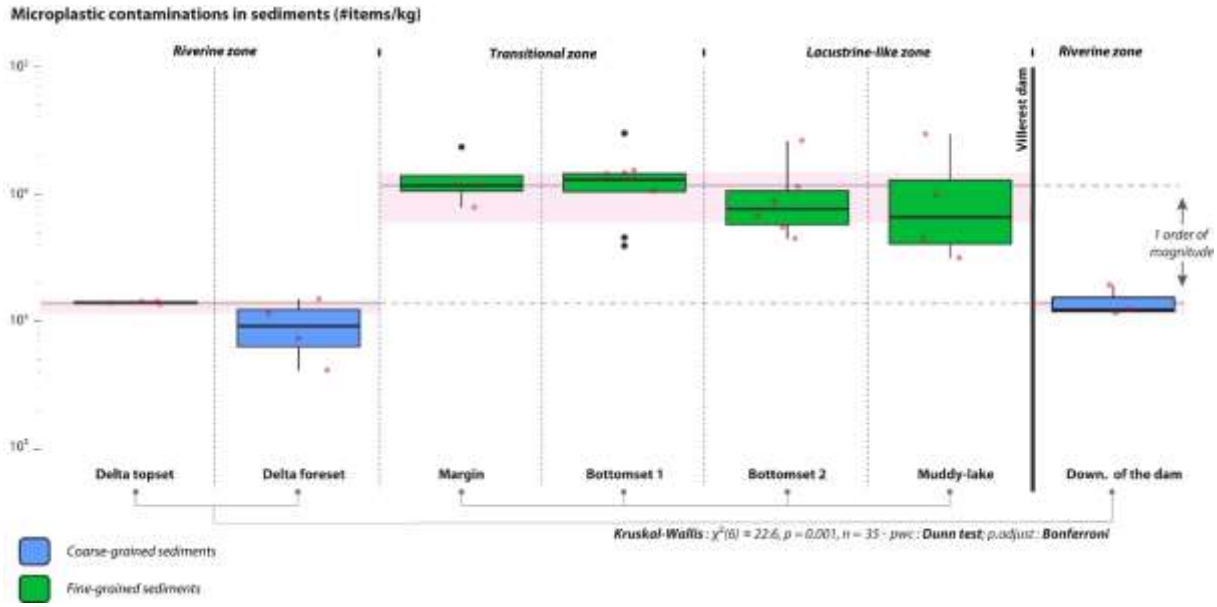

Fig. 3: Statistical distribution of the total microplastic contents in sediments regarding each geomorphic structure of the reservoir. A nonparametric statistical analysis highlights two groups (p value < 0.05), corresponding to coarse-grained and fine-grained deposits. Grey lines and envelopes represent the 50, 25 and 75% percentiles in these two groups.

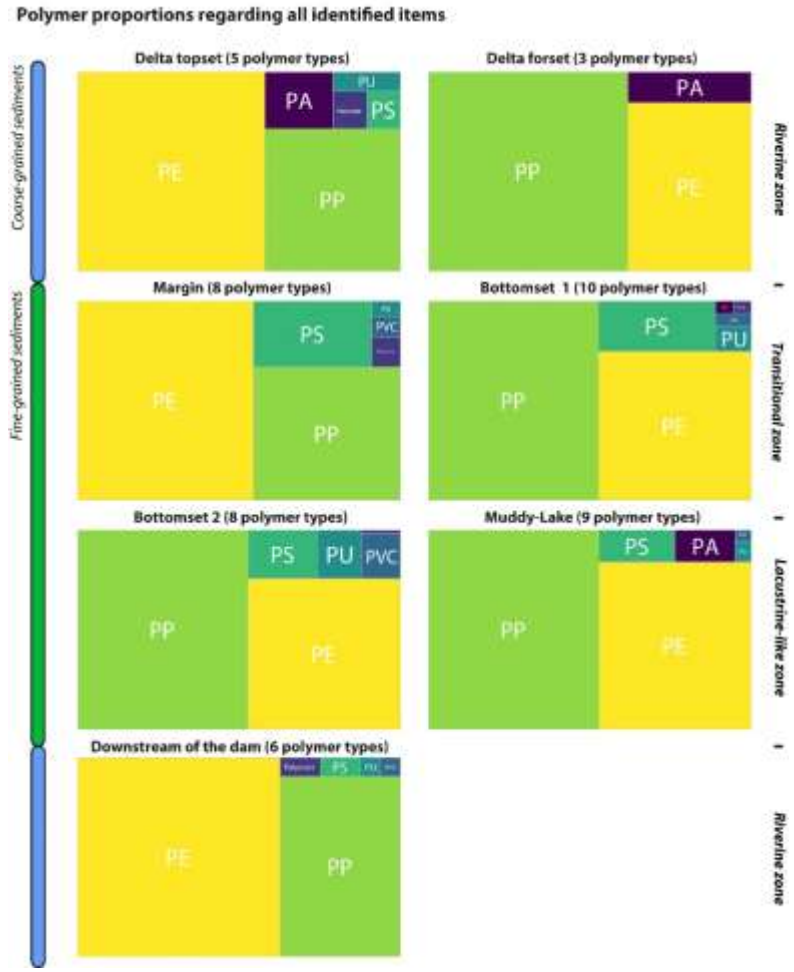

Fig. 4: Statistical classification of polymers by order of proportions regarding all microplastics typified in each geomorphic structure of the reservoir (*PP = polypropylene, PE = polyethylene, PS = polystyrene, PA = polyamide, PU = polyurethane, PVC = polyvinylchloride*).

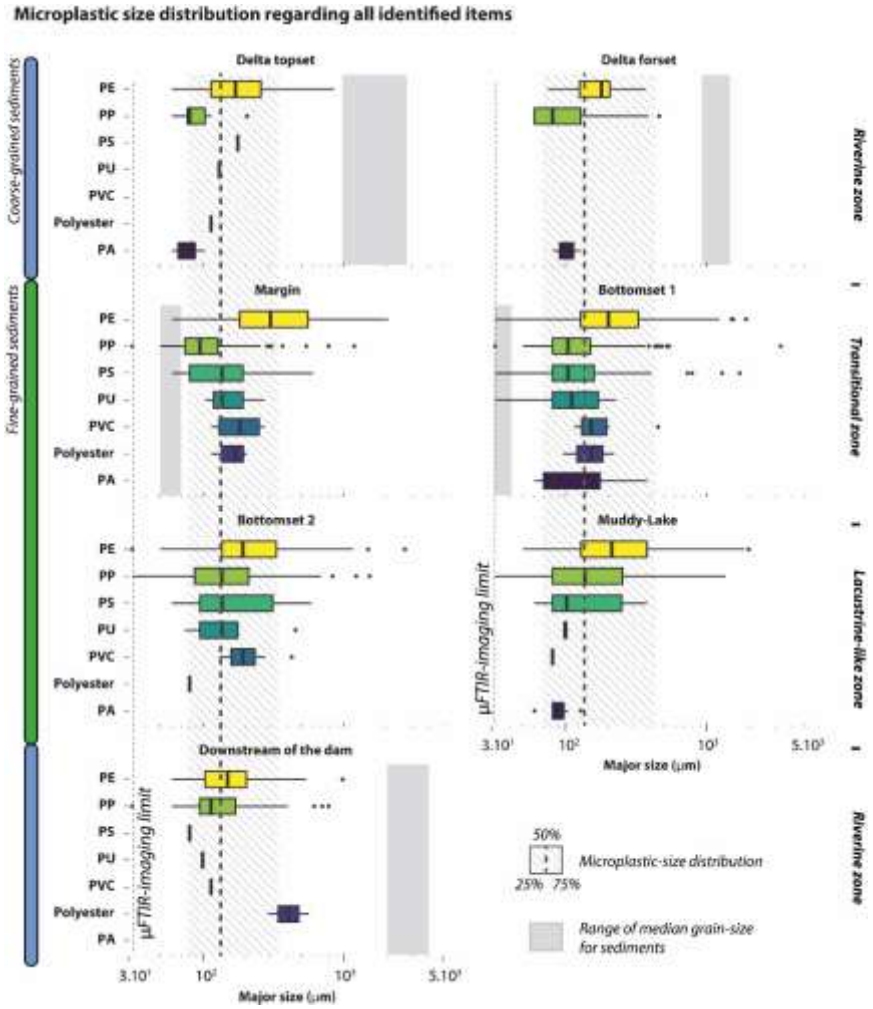

Fig. 5: Microplastic size distribution according to the polymer composition in each geomorphic structure of the reservoir. The minimum particle size measured by the µFTIR imaging is 32 µm (*PP = polypropylene, PE = polyethylene, PS = polystyrene, PA = polyamide, PU = polyurethane, PVC = polyvinylchloride*).

	Coarse-grained sediments			Fine-grained sediments		
R-value (Pearson correlation)	pp	pe	ps	pp	pe	ps
< 2 µm (Clay)	-	-	-	*-0.09*	*-0.42*	**-0.60**
< 10 µm (Finest fraction)	*-0.11*	*0.27*	*0.60*	*-0.07*	**-0.50**	**-0.61**
< 63 µm (Mud)	*-0.10*	*0.17*	*0.67*	*-0.02*	*-0.37*	*-0.41*
63-2 000 µm (Sand)	*-0.05*	*0.27*	*-0.29*	*0.02*	*0.37*	*0.41*
TOC content	*0.07*	*0.27*	*0.29*	*0.29*	*0.06*	*-0.21*

Table 1: Pearson correlations (R-value) calculated between the MP contents *(#items/kg)* and sediment grain-size parameters *(%)* and TOC contents *(%)*. The three most abundant polymers are presented here. Significant correlations are shown in bold (p value < 0.05).